CHAPTER 9

RESULTS AND DISCUSSION: COMPARISON OF PHOSPHATE REMOVAL BY FLY ASH, SLAG, OPC, OPC/FA AND OPC/SLAG

9.1. Chemical composition and particle dimensions

The chemical oxide composition of FA, slag and OPC, obtained by XRF, are shown in Table 9.1.

Table 9.1. Chemical composition of FA, slag and OPC.

	Mass %		
	FA	Slag	OPC
SiO_2	52.4	33.4	22.5
Al_2O_3	33.7	11.0	4.5
Fe_2O_3	3.6	0.7	1.4
Mn_2O_3	<0.1	0.4	0.9
TiO_2	1.7	0.6	0.2
CaO	4.1	33.3	63.2
MgO	1.1	18.0	3.6
P_2O_5	0.3	0.0	0.2
SO_3	0.2	0.6	2.4
Cl	<0.1	<0.1	<0.1
K_2O	0.6	0.3	0.8
Na_2O	0.5	0.2	0.1
LOI	0.8	1.7	1.0
Total	99.0	100.2	100.8
CaO/SiO_2	0.08	1.00	2.81

The theoretical total is 100 % and the difference between this and the actual total reported is an indication of both the accuracy of the analysis and the possible existence of elements in the sample that had not been analysed for. LOI (loss on ignition) is the mass loss caused by materials vaporised during the heating of the sample to a temperature of 1000 °C for a period of about 30 minutes. Calculated values for lime-silica ratios (CaO/SiO_2) are included in Table 9.1. The high CaO/SiO_2 ratio for OPC compared to slag and fly ash reflects the greater tendency for the former to undergo cementitious reactions (e.g. hydration).

Table 9.2 contains a summary of some important physical properties obtained by Fraunhofer particle diffraction analysis.

Table 9.2. Physical characteristics of FA, slag and OPC.

Characteristic	Value		
	FA	Slag	OPC
Specific surface area (m^2/g)	1.42	1.29	1.38
Mean particle diameter (μm)	25.7	31.4	20.8
Density (g/cm^3)	2.21	2.82	3.02

It can be seen from Table 9.2 that the specific surface areas (1.4, 1.3 and 1.4 m^2/g respectively) of the fly ash, slag and OPC samples used for the study are quite similar. One would therefore expect them to exhibit somewhat similar adsorption

capacities if physical adsorption at the surface of the sorbent particles is the sole or principal contributory phenomenon to solute removal, other factors being equal.

9.2. Kinetics

Figure 9.1 illustrates the variation of percentage removal of PO_4^{3-} with time for the different adsorbents. It can be seen that OPC removed PO_4^{3-} at the fastest rate and fly ash the slowest. The uptake of PO_4^{3-} by OPC virtually ceased after a contact time of about 3 h, compared to about 6 h for fly ash, with 84 and 34 percent PO_4^{3-} removal at equilibrium, respectively.

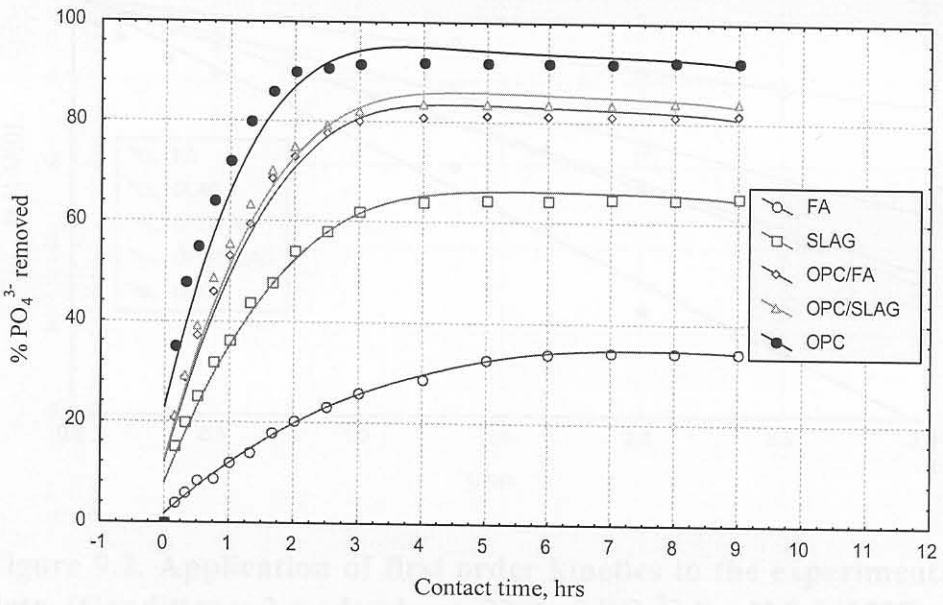

Figure 9.1. Kinetics of PO_4^{3-} removal by the adsorbents. (Conditions: 2 g adsorbent, 80 mg/l PO_4^{3-}-P, pH 9.0, 25°C)

Blending of OPC with fly ash or slag was observed to lead to an overall decrease in the rate and efficiency of PO_4^{3-} removal. Although slag removes PO_4^{3-} better than fly ash, 19 % replacement of OPC with slag evidently results in a blend with a lower PO_4^{3-} removal efficiency than 11 % replacement with fly ash.

Curves plotted according to equation (1.12) are presented in Figure 9.2. The good straight-line fits observed (linear correlation coefficients $R^2 \geq 0.99$) indicates that the sorption reactions may be approximated by first-order reversible kinetics; the calculated rate constants are given in Table 9.3.

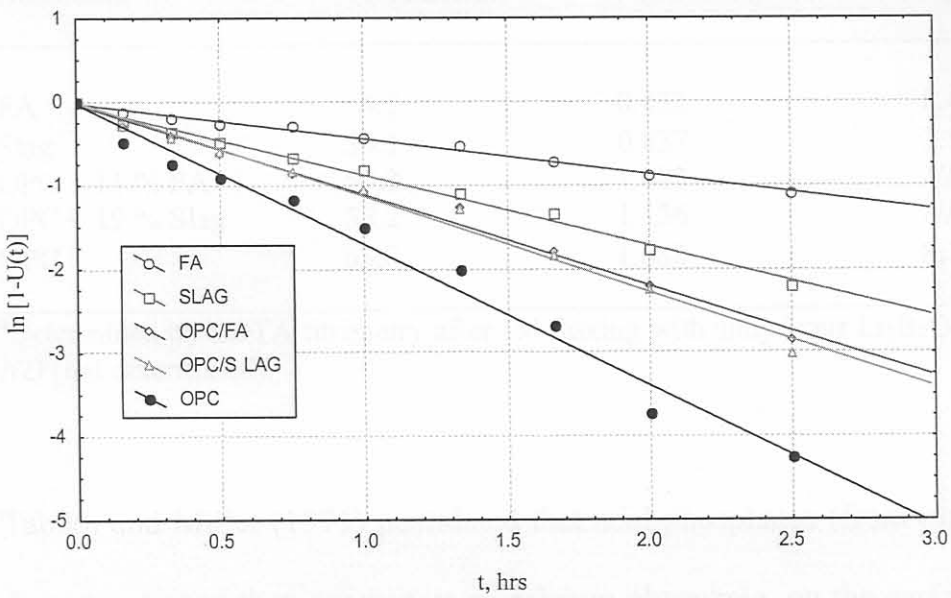

Figure 9.2. Application of first order kinetics to the experimental adsorption data. (Conditions: 2 g adsorbent, 80 mg/l PO_4^{3-}-P, pH 9.0, 25°C)

Over the range of sorbent-solution agitation rates studied (100-140 cycles per minute horizontally) it was observed that the sorption rate was not affected by the

rate of mixing. This suggests that diffusion through the pores of sorbent particles rather than diffusion to the film at the sorbent particle-aqueous solution interface were rate limiting, which would provide evidence that intra-particle diffusion is the controlling resistance rather than external diffusion. The values of intra-particle diffusion constants calculated using equation (1.13) are given in Table 9.3. The value obtained for OPC was an order of magnitude greater than that for fly ash.

Table 9.3. The values of first order reaction rate constants and intra-particle diffusion coefficients.

Adsorbent	% CaO[a]	k' (per hour)	D (cm^2/s)
FA	4.5	0.423	8.40×10^{-12}
Slag	34.1	0.837	2.51×10^{-11}
OPC + 11 % FA	57.3	1.082	*ND*
OPC + 19 % Slag	58.2	1.136	*ND*
OPC	63.8	1.682	8.72×10^{-11}

[a]Determined by EDTA titrimetry after 1:4 fluxing with anhydrous $Li_2B_4O_7$.
ND (not determined).

Tabikh and Miller (1971) postulated that acid phosphates (from phosphogypsum) deprotonate and then precipitate as calcium phosphate, on the surface of the grain in the alkaline region in the immediate vicinity of a hydrating particle. This provides a protective barrier against attack by water, resulting in the delayed setting times observed. Hence, the affinity of phosphate (the adsorbate, from the acid phosphate KH_2PO_4) for CaO (in the adsorbent) observed in this study is

hardly surprising. This would also explain the reason why pre-treatment of the phosphogypsum by washing with milk of lime (Erdogan et. al., 1994) was successful in minimising the effect on setting time extension.

9.3. Effect of concentration

The rate and separation efficiency of PO_4^{3-} from aqueous solution by these adsorbents was found to increase with the initial phosphate concentration over the concentration range studied (see Figures 5.6, 6.5 and 7.4); this is indicative of a non-ideal system, as explained in Section 5.4. Changes in concentration alone did not appear to significantly affect the time required for PO_4^{3-} adsorption to reach equilibrium.

9.4. Effect of particle size

Figure 9.3 shows the effect of particle size on the efficiency of PO_4^{3-} removal by fly ash, slag and OPC. Although there was some increase in the percentage PO_4^{3-} removed as the adsorbent particle size decreased, this increase was not proportional to the increased surface area. This diminished effect of increasing surface area on the percentage PO_4^{3-} removed is an indication that for these

adsorbents physical adsorption at the surface of the sorbent particles is probably not the sole phosphate removal mechanism.

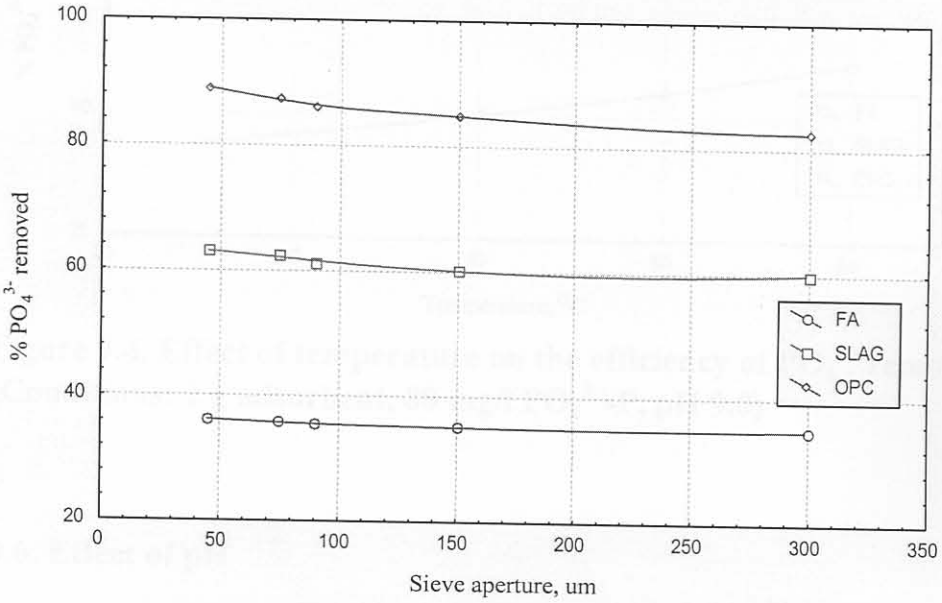

Figure 9.3. Effect of particle size on the efficiency of PO_4^{3-} removal. (Conditions: 2 g adsorbent, 80 mg/l PO_4^{3-}-P, pH 9.0, 25°C)

9.5. Effect of temperature

The effect of temperature on the efficiency of PO_4^{3-} removal by fly ash, slag and OPC is illustrated in Figure 9.4. The percentage PO_4^{3-} removed was observed to increase with increasing temperature. This is not surprising, since the rate of intra-particle diffusion (see Section 9.2) is expected to increase with increasing temperature.

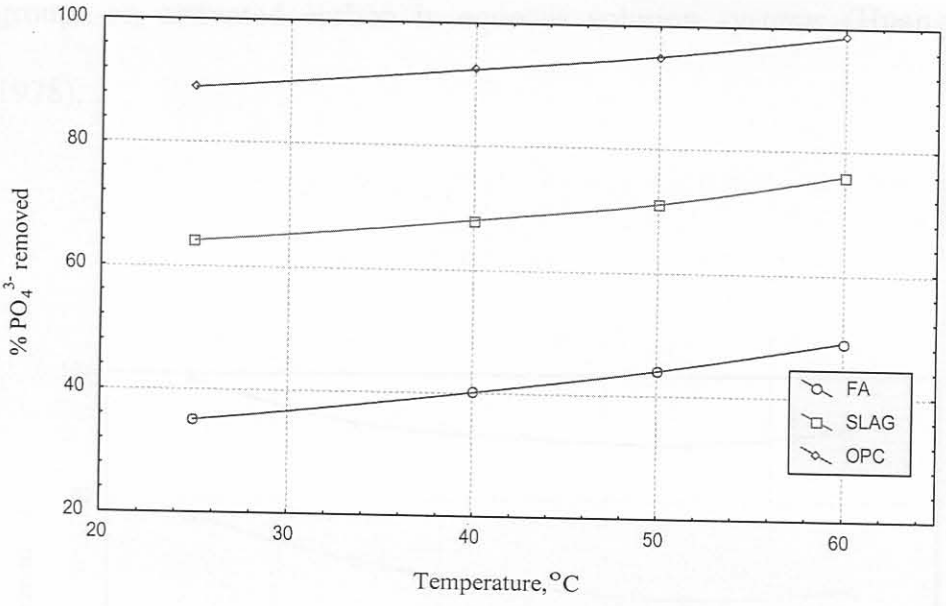

Figure 9.4. Effect of temperature on the efficiency of PO_4^{3-} removal. (Conditions: 2 g adsorbent, 80 mg/l PO_4^{3-}-P, pH 9.0)

9.6. Effect of pH

Figure 9.5 illustrates the variation of percentage PO_4^{3-} removed with the initial pH of the aqueous solution that was added to fly ash, slag and OPC. It can be seen from the figure the efficiency of PO_4^{3-} removal increases steadily in acidic pH. This is probably due to the accumulation of positive charge on the adsorbent surface (at low pH) that increases its affinity for the negatively charged phosphate ions. Some of the oxides (especially those of Al and Si) in these sorbents can be expected to form hydroxide complexes in aqueous solution whose basic or acidic dissociation may lead to an accumulation of net positive or negative charge at the solid-solution interface. Similar behaviour has been reported for surface hydroxo

groups on activated carbon in aqueous solution systems (Huang and Ostovic, 1978).

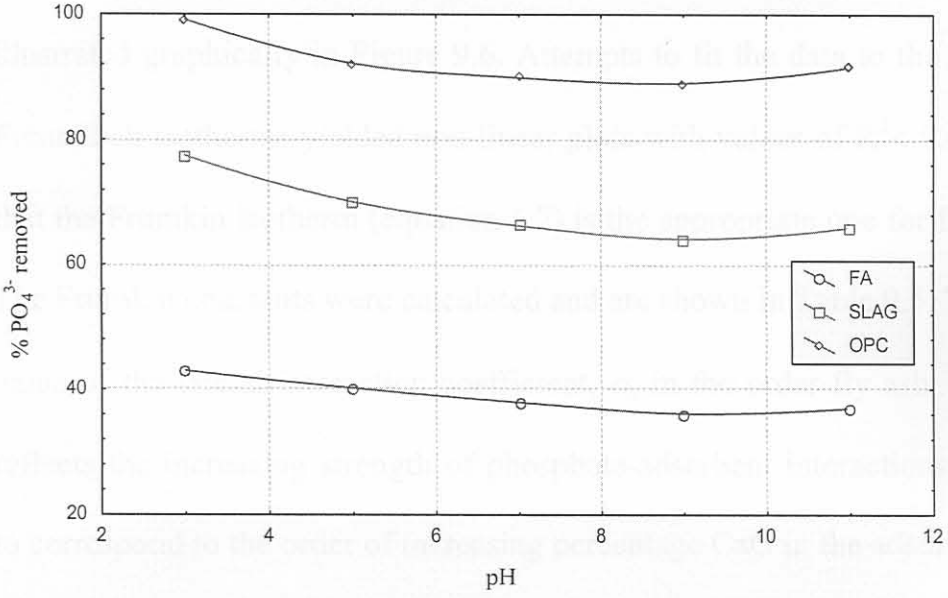

Figure 9.5. Effect of pH on the efficiency of PO_4^{3-} removal. (Conditions: 2 g adsorbent, 80 mg/l PO_4^{3-}-P, 25°C)

The observed slight increase in the efficiency of PO_4^{3-} removal beyond pH 9 could be due to the creation of favourable conditions for calcium phosphate precipitation at high pH, thus enhancing the removal of PO_4^{3-} by dissolved calcium formed by hydration of the adsorbent.

9.7. Adsorption isotherms

Table 9.4 shows the experimentally obtained adsorption data for fly ash, slag and OPC. The fit of these data to the Frumkin isotherm (see equations 1.6 & 1.7) are shown in Table 9.5, and the application of the Frumkin equation to the data is illustrated graphically in Figure 9.6. Attempts to fit the data to the Langmuir and Freundlich isotherms yielded non-linear plots with values of $R^2 < 0.4$. It is evident that the Frumkin isotherm (equation 1.7) is the appropriate one for fitting the data. The Frumkin constants were calculated and are shown in Table 9.5. The increasing value of the lateral interaction coefficient, α, in the order fly ash, slag and OPC reflects the increasing strength of phosphate-adsorbent interactions. This appears to correspond to the order of increasing percentage CaO in the adsorbents.

Table 9.4. Experimental adsorption data for FA, slag and OPC.

	FA		Slag		OPC	
Mass of adsorbent (g)	P^a after adsorption (mg/l)	P^a adsorbed (mg)	P^a after adsorption (mg/l)	P^a adsorbed (mg/l)	P^a after adsorption (mg/l)	P^a adsorbed (mg)
0.5	72.8	5.44	48.5	10.3	34.4	13.1
2	71.9	5.62	46.7	10.6	32.2	13.6
3	71.4	5.72	45.8	10.8	31.1	13.8
3.5	70.2	6.43	43.5	11.3	28.2	14.4
4	65.0	7.00	33.7	13.3	15.6	16.9
5	58.7	8.26	21.7	15.7	0.4	19.9

[a] PO_4^{3-} (as P)

Table 9.5. Isotherm constants and linear correlation coefficients for FA, slag and OPC.

Adsorbent	Freundlich R^2	Langmuir R^2	Frumkin		
			R^2	α	β
FA	0.2793	0.3763	0.9918	3.061	0.0254
Slag	0.2333	0.2687	0.9974	3.780	0.0149
OPC	0.1385	0.2699	0.9945	4.976	0.0042

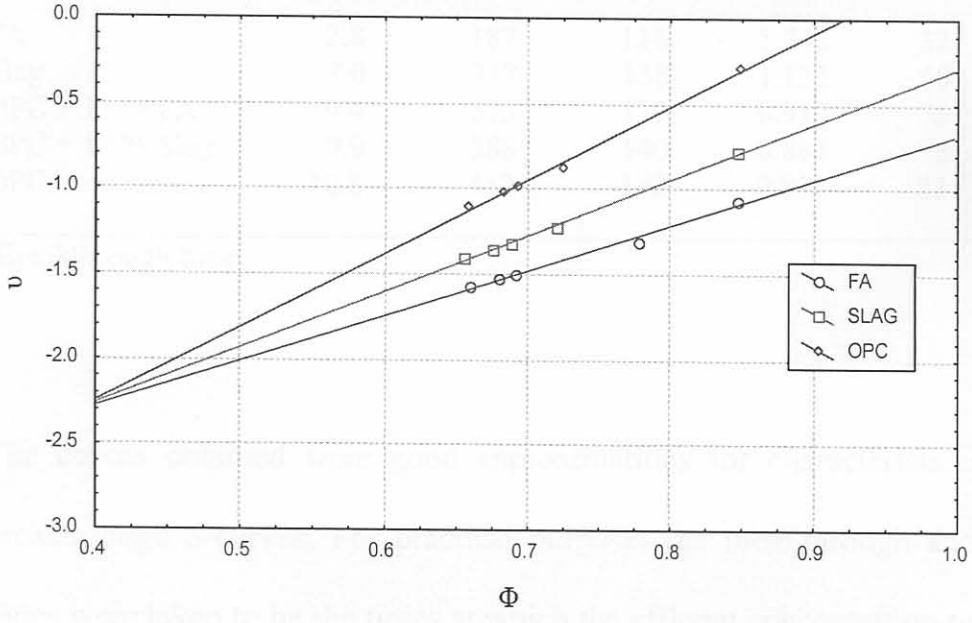

Figure 9.6. Application of the Frumkin equation to the experimental adsorption data (given in Table 9.4) for FA, slag and OPC.

It must be pointed out that magnesium, like calcium, will also dissolve to a certain extent and contribute to the observed PO_4^{3-} removal. However, this contribution appears to be relatively minor, considering the fact that slag contains nearly six times as much MgO as OPC (see Table 9.3).

9.8. Breakthrough curves

The data obtained for the breakthrough experiments for the various adsorbents are shown in Table 9.6, and typical breakthrough curves are represented in Figure 9.7.

Table 9.6. Breakthrough data for FA, slag, OPC, OPC/FA and OPC/slag.

Adsorbent	t_E[a] (min)	V_T (cm^3)	V_Z (cm^3)	h_Z (cm)	C_T (mg PO_4^{3-}-P/g)
FA	2.8	187	116	1.742	32
Slag	7.0	312	138	1.133	60
OPC + 11 % FA	9.4	375	139	0.910	75
OPC + 19 % Slag	9.9	388	140	0.881	78
OPC	10.8	412	142	0.833	83

[a]Breakthrough time

The curves obtained were good approximations for characteristic symmetrical breakthrough *S*-curves. For practical purposes the breakthrough and exhaustion times were taken to be the times at which the effluent concentration reached 5 and 95 %, respectively, of the influent concentration.

The value of the height of the exchange zone h_Z decreases in the order: fly ash, slag, OPC/fly ash, OPC/slag, OPC. This is a measure of increasing rate of ion exchange and/or phosphate removal, while the increasing value of the breakthrough time t_E is indicative of increasing adsorption capacity. These

experimentally obtained (by graphical integration of Eq.(1.16) values may be extrapolated to estimate the capacity of a large-scale bed (Helfferich, 1962).

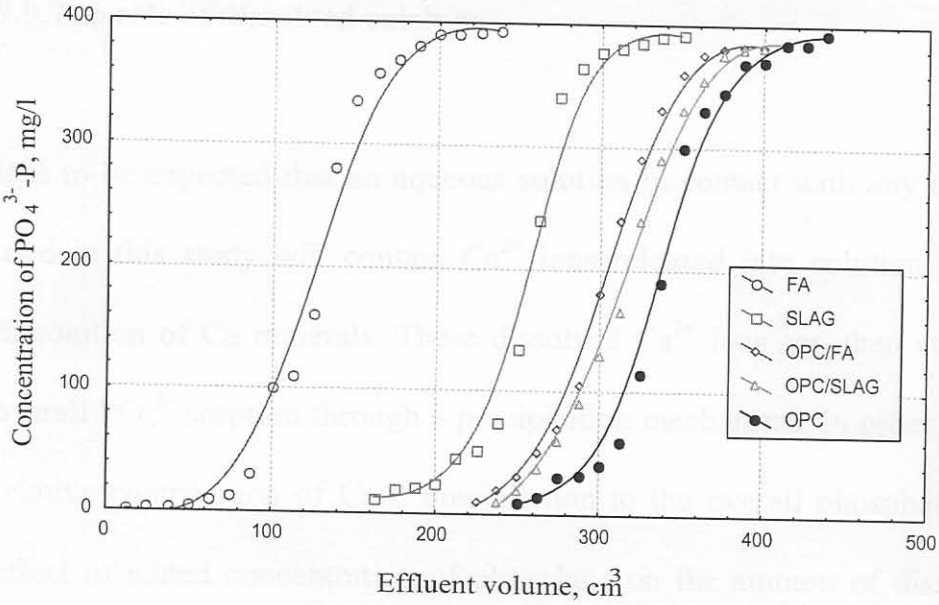

Figure 9.7. Breakthrough curves for PO_4^{3-} removal by FA, slag, OPC, OPC/FA and OPC/slag.

The value of 32 mg/g obtained in this study for phosphate adsorption on fly ash is of the same order of magnitude as the 67 mg/g reported by Akgerman and Zardkoohi (1996) for the adsorption of phenol on an American fly ash. Sakadevan and Bavor (1998) reported a value of 44.2 mg/g for phosphate adsorption on slag, compared to the 60 mg/g obtained in this study. It must be pointed out that Sakadevan and Bavor (1998) followed the common practise of calculating adsorption capacity from the best-fit adsorption isotherm. The breakthrough

curves approach used in this study, although more time-consuming, offers a more direct experimental determination.

9.9.The role of dissolved calcium

It is to be expected that an aqueous solution in contact with any of the materials used in this study will contain Ca^{2+} ions released into solution through partial dissolution of Ca minerals. These dissolved Ca^{2+} ions can then contribute to the overall PO_4^{3-} sorption through a precipitation mechanism. In order to estimate the relative contribution of Ca-P precipitation to the overall phosphate sorption, the effect of added concentration of phosphate on the amount of dissolved calcium was investigated.

9.9.1. Procedure

2 g of sorbent were shaken continuously with 200 ml of 0, 20, 40, 60 and 80 mg/l PO_4^{3-}-P solution (initial pH 9.0, 25°C) for 10 hours, after which the concentration of calcium in the filtered (45-µm membrane) supernatant solution was measured by flame atomic absorption spectrometry. A Varian SpectrAA220 instrument supplied by SMM Instruments (Pty) Limited, Johannesburg, was used. The experimental conditions used were as follows: flame: N_2O-C_2H_2, lamp current: 10 mA, λ: 422.7 nm, slit width: 0.5 nm.

9.9.2. Results and discussion

The observed effect of added concentration of phosphate on the amount of dissolved calcium is shown in Figure 9.8.

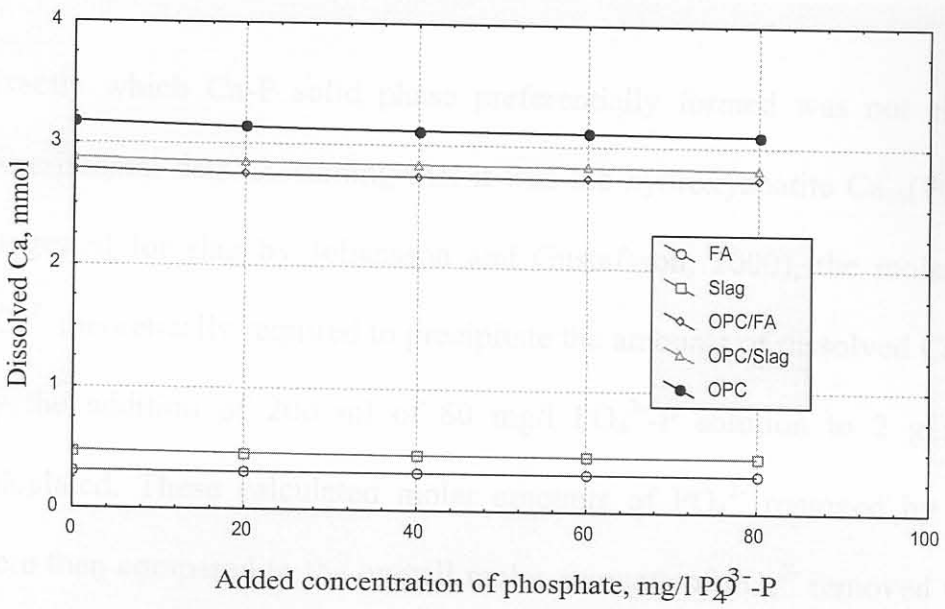

Figure 9.8. Effect of added concentration of phosphate on the amount of dissolved calcium.

(Conditions: 2 g sorbent, 200 ml PO_4^{3-} solution, pH 9.0, 25°C)

The amount of dissolved calcium decreased as the initial concentration of the added phosphate solution increased. This was taken as evidence for Ca-P precipitation. This phenomenon appears to be relatively more pronounced for OPC

and its blends than it is for slag and FA, which is hardly surprising. OPC is expected to release more Ca^{2+} ions into solution via dissolution since it contains a larger amount of Ca to start with (see Table 9.1), and also has a greater tendency to undergo hydration, which releases additional into solution (see Equations 2.3 and 2.4).

Exactly which Ca-P solid phase preferentially formed was not clear from the experimental data. Assuming that it was the hydroxyapatite $Ca_{10}(PO_4)_6(OH)_2$ (as suggested for slag by Johansson and Gustafsson, 2000), the molar amounts of PO_4^{3-} theoretically required to precipitate the amounts of dissolved Ca^{2+} consumed by the addition of 200 ml of 80 mg/l PO_4^{3-}-P solution to 2 g sorbent were calculated. These calculated molar amounts of PO_4^{3-} removed by precipitation were then compared to the overall molar amounts of PO_4^{3-} removed when 200 ml of 80 mg/l PO_4^{3-}-P solution is added to 2 g sorbent (see Figure 9.1), to obtain estimates for the percentage of PO_4^{3-} removed by Ca-P precipitation. The results are shown in Table 9.7.

Table 9.7. Estimated relative contribution of Ca-P precipitation to the overall phosphate sorption.

Sorbent	Mol PO_4^{3-} removed		% PO_4^{3-} removal by Ca-P precipitation
	Overall	By Ca-P precipitation	
FA	1.8×10^{-4}	2.1×10^{-6}	1.2
Slag	3.3×10^{-4}	1.6×10^{-5}	4.8
OPC+11% FA	4.2×10^{-4}	3.6×10^{-5}	8.6
OPC+19% Slag	4.3×10^{-4}	3.8×10^{-5}	8.8
OPC	4.7×10^{-4}	4.6×10^{-5}	9.8

As can be seen from the entries in the table, the molar amounts of phosphate removed by Ca-P precipitation are one (two in the case of fly ash) order of magnitude smaller than the overall amounts sorbed. Similar results were obtained when the calculations were repeated for other known Ca-P solid phases, such as tricalcium phosphate $Ca_3(PO_4)_2$, amorphous calcium phosphate $Ca_4H(PO_4)_3$ and brushite $CaHPO_4.2H_2O$. The contribution of Ca-P precipitation appears to be only marginal for fly ash, and even for OPC is less than ca.10 %.

Adsorption is evidently the major contributing mechanism to the overall phosphate removal. There are other observations that would be difficult to explain if precipitation were the major contributing mechanism compared to adsorption. Firstly, the process follows first order kinetics and takes several hours to reach completion, whereas precipitation reactions are typically much faster. Secondly,

the experimental data fits the Frumkin adsorption isotherm very closely. Thirdly, phosphate removal efficiency increases with increasing temperature. If precipitation were dominant, an increase in temperature would probably result in re-dissolution of precipitate and hence decreased phosphate removal. Fourthly, more phosphate is removed at lower pH. The solubility of the Ca-P solid phase is expected to decrease at lower pH due to decreased concentration of phosphate, so less phosphate removal would be expected at low pH.

9.10. Report on production of bricks

The possibility of producing bricks from a bed of sand and OPC, OPC/slag or OPC/FA, after being used to remove phosphate from aqueous solution, was investigated as a possible added-value application.

9.10.1. Procedure

A 20-mg/l PO_4^{3-}-P aqueous solution, sand and OPC, OPC/FA or OPC/slag were weighed (the calculated amounts are shown in Table 9.8.) and mixed to uniform consistency. The mixtures were poured into 7 cm × 7 cm × 7 cm lubricated moulds and air bubbles removed by vibration. The moulds were placed in plastic containers under a water vapour saturated atmosphere for 1 day, after which they were removed and placed in water for specified curing periods. The bricks were

tested for their compressive strengths within 5 min of their removal from water, according to the standard method for concrete masonry units in South Africa (SABS, 1984). This involved placing the brick correctly on the testing machine, applying a pre-load of 5 kN (without shock) to the brick and then increasing the load at a uniform stress rate of about 15 MPa/min until the brick failed. The failure load was recorded and used to calculate the compressive strength. The testing machine used was a Farnell press (D. Kind laboratory Supplies, Johannesburg).

9.10.2. Data and calculations

The mix proportions and calculated amounts of constituents required for the mixtures used to produce the test bricks are shown in Table 9.8.

Table 9.8. Mix proportions used for producing test bricks.

Mixture	Sand : OPC	Amounts				
		Water (cm^3)	Sand (g)	OPC (g)	FA (g)	Slag (g)
1	1 : 2	214	237.4	474.8	-	-
2	1 : 2 + 15% FA	214	130.6	474.8	106.8	-
3	1 : 2 + 15% slag	214	130.6	474.8	-	106.8

Water to cement ratio, W/C = 0.3

9.10.3. Results and discussion

The strength of the bricks produced according to the mix proportions shown in Table 9.8 are given in Table 9.9.

Table 9.9. Brick compressive strength.

Mixture	Curing period (days)	Compressive Strength (kN)	(MPa)[a]
1	2	37	7.6
	7	80	16.3
	14	120	24.5
	28	180	36.7
2	2	35	7.1
	7	60	12.2
	14	90	18.4
	28	120	24.5
3	2	20	4.1
	7	35	7.1
	14	50	10.2
	28	95	19.4

[a] 1 Pa = 1 N/m^2, Area of a brick = 7 cm × 7 cm = 0.0049 m^2

Figure 9.9 illustrates the strength development graphically. The compressive strengths of the water-cured bricks were found to increase in the order OPC/slag, OPC/fly ash, OPC. In South Africa bricks must meet a minimum compressive strength requirement of 7.0 MPa after 28 days (SABS, 1984) before they can be approved for building purposes. The results clearly show that the bricks produced

and tested in this study more than meet this requirement, even after just 7 days of curing.

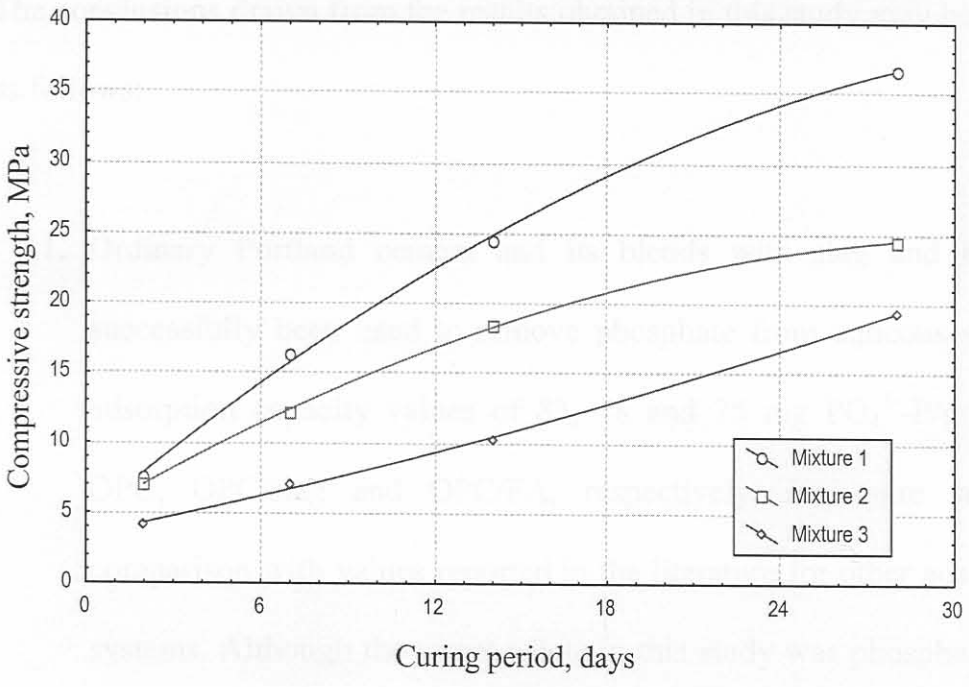

Figure 9.9. Strength development in the bricks produced.